Journal of the Korean Ceramic Society
Vol. 31, No. 10, PP. 1147~1158, 1994.

Preparation of $MgO-ZrO_2$ Fibers by Sol-Gel Method and Their Characterization

Chin-Myung Whang and Hee-Tai Eun
Dept. of Ceramic Engineering, Inha University
(Received June 15, 1994)

졸-겔법에 의한 $MgO-ZrO_2$ 섬유의 제조와 특성

황진명 · 은희태
인하대학교 무기재료공학과
(1994년 6월 15일 접수)

ABSTRACT

From $Zr(O\text{-}nC_3H_7)_4$-H_2O-C_2H_5OH-HNO_3 starting solutions, MgO-doped stabilized zirconia fibers with varying content of MgO (10~18 mol%) from different MgO sources were fabricated by sol-gel method. The MgO sources used are magnesium nitrate hexahydrate, magnesium acetate tetrahydrate, and magnesium ethylate. The phase transformation studies of a drawn $MgO-ZrO_2$ fiber were carried out using X-ray diffraction, IR spectroscopy, and Raman spectroscopy. The microstructure, tensile strength, and microporosity of fibers were investigated using SEM, tensile strength test, and microporosimeter. Although various MgO sources such as magnesium nitrate, acetate, and ethylate were used, the crystallization behavior of $MgO-ZrO_2$ fibers at different temperatures could be summarized as follows: Cubic→Metastable Tetragonal→Monoclinic→Coexistence of Monoclinic and Cubic→Cubic(trace of monoclinic). At 1500℃, the phase transformation of $MgO-ZrO_2$ fibers shows the following change depending on the amount of $MgO[Mg(NO_3)_2\cdot 6H_2O]$: At 10 mol%, both monoclinic and cubic phase coexist, at 12 mol%, monoclinic phase decreases rapidly, and then at 14 mol%, only cubic phase remains. When the $MgO-ZrO_2$ fibers containing 12 mol% magnesium nitrate were heated at 800℃ for 1hr, average tensile strength of fibers is 4.0 GPa at diameters of 20 to 30 μm. As the heat-treatment temperatures increase to 1000℃ for 1 hr, tensile strength of $MgO-ZrO_2$ fibers decreases rapidly to 0.7 GPa.

요 약

졸-겔법을 이용, $Zr(O\text{-}nC_3H_7)_4$-H_2O-C_2H_5OH-HNO_3 용액을 출발물질로하여 안정화제로 MgO를 첨가하고 여러 종류의 MgO 출발물질 및 MgO의 첨가량을 10~18 mol% 범위에서 변화시킨 zirconia 섬유를 제조하였다. MgO의 출발물질로서는 magnesium nitrate hexahydrate, magnesium acetate tetrahydrate, magesium ethylate를 사용하였다. 제조된 $MgO-ZrO_2$ 섬유의 상전이에 대한 연구는 X-선 회절분석, IR 분광분석 및 Raman 분광분석을 통하여 이루어졌고, 미세구조관찰 및 인장강도와 미세기공을 측정하였다. MgO 출발물질이 magnesium nitrate, acetate 및 ethylate로 변화하여도 열처리 온도변화에 따른 $MgO-ZrO_2$ 섬유의 상전이는 입방정상→준안정 정방정→단사정상→단사정상과 입방정상의 공존→입방정상(단사정상의 흔적)으로 진행되었다. 1500℃ 에서 $MgO[Mg(NO_3)_2\cdot 6H_2O]$의 첨가량에 따른 상전이는 10 mol%에서는 단사정상과 입방정상이 공존하나 12 mol%에서는 단사정상이 급격히 감소하였으며, 14 mol% 이상에서는 입방정상만 존재하였다. 안정화제로 magnesium nitrate가 12 mol% 첨가된 섬유를 800℃, 1시간 열처리 하였을 경우, 섬유는 20~30 μm의 직경에서 4.0 GPa의 우수한 강도를 나타내었으며, 열처리 온도가 1000℃ 로 증가함에 따라 섬유의 인장강도는 0.7 GPa로 급격히 감소하였다.

1. Introduction

Zirconia ceramics have three well-known polymorphic forms-monoclinic, tetragonal, and cubic- and characteristically they transform between phases depending on the temperatures under atmospheric pressure. Also, zirconia exhibits excellent mechanical properties such as high temperature strength and therefore, con-

siderable attention has been given to MgO-, CaO-, and Y_2O_3-doped partially stabilized zirconia for their use as a structural material because of high strength and high toughness[1-3].

Among these partially stabilized zirconia, especially widely used transformation-toughened ceramics are based on magnesia-partially stabilized zirconia. These materials are characterized by a well-defined microstructure consisting of cubic matrix containing a second phases of finely dispersed submicrometer tetragonal. Transformation toughening in Mg-PSZ results from the fact that when tetragonal dispersed in cubic is subjected to outside stress, tetragonal to monoclinic transformation absorbs stress-energy, maintaining the high strength.

Consequently, Mg-PSZ has various applications such as dry-bearing, nozzle, extrusion die, components in diessel engines, and biomaterials. And if these materials were made to fiber form, it could be used for refractories, catalyst conductors reinforcements for metals, and ceramics as well as potential uses in industrial areas[4-6].

Until now, because of their high melting point, zirconia fibers cannot be fabricated by the melt process. Accordingly, many methods are under investigation to manufacture the zirconia fibers[7-11]. Among these methods, fiber preparation using sol-gel process has attracted a considerable attention because of its many excellent characteristics. Y_2O_3- and CaO-doped zirconia fibers prepared by sol-gel process were reported to have high tensile strength above 1 GPa[8,10,11,19].

The preparation of MgO-doped zirconia fibers reported thus far are the following two cases. In one method, the zirconia fibers are spun out of zirconium acetate or chloride solutions containing 7 mol% magnesium acetate or chloride in proper viscosity. In the other method, it is spun from polyzirconosane solutions with 4 wt% magnesium acetylacetonate using rotational spinner[12,13]. Also, Yermolenko et al.[14] reported to have manufactured the zirconia fibers from zirconium salt solution with magnesium salt ranging 5 to 30 mol% as a starting material.

But, in previous studies, they only fabricated the fibers and no systematic researches have been carried out as to various experimental factors affecting fiber synthesis, phase transformation accompanying to heat treatment, microstructure and tensile strength of fiber.

The preparation of MgO-ZrO_2 fibers using zirconium alkoxide have not been reported, either. Also, the phase transformation affecting the property of zirconia fiber depends markedly on the manufacturing process and on the content and type of dopants.

The object of this study is to prepare MgO-ZrO_2 fibers using zirconium n-propoxide and MgO by sol-gel process and to investigate the effect of the phase transformation of MgO-ZrO_2 fibers, systematically, as MgO sources were varied to magnesium nitrate, acetate, and ethylate. Also, studies on phase transformation of MgO-ZrO_2 fibers depending on the amounts of MgO and heat treatment temperatures were carried out by means of X-ray diffraction and vibrational spectroscopy (FT-IR and Raman). Raman spectroscopy is a very useful tool for phase identification of zirconia because the Raman modes assigned to the tetragonal phase and the monoclinic phase are distinctively apparent.

We have also investigated the microstructure of fibers by SEM and measured the tensile strength of drawn MgO-ZrO_2 fibers.

2. Experimental

2.1. The preparation of MgO-ZrO_2 fibers

In this work, zirconium n-propoxide[$Zr(O\text{-}nC_3H_7)_4$, Fluka], magnesium nitrate hexahydrate[$Mg(NO_3)_2 \cdot 6H_2O$, Fluka; abbreviated as Mg(N)], magnesium acetate tetrahydrate[$Mg(CH_3CO_2)_2 \cdot 4H_2O$, Aldrich; abbreviated as Mg(A)], and magnesium ethylate[$C_4H_{10}MgO_2$, Fluka; abbreviated as Mg(E)] were used for MgO-ZrO_2 fiber preparation.

The MgO-ZrO_2 fibers are prepared according to the flow diagram shown in Fig. 1. 1.2 M $Zr(O\text{-}nC_3H_7)_4$-C_2H_5OH solutions were measured in glove box under N_2 atmosphere and stirred in a waterbath at 25℃ for 1 hr. The other mixed solution of C_2H_5OH-HNO_3-Mg(N), Mg(A), or Mg(E) was added dropwise to the $Zr(O\text{-}nC_3H_7)_4$-C_2H_5OH solution using a syringe.

The prepared sol solutions were divided into PE tubes, their pH measured and then concentrated at 80℃ for 6 hrs using a waterbath and kept open in ambient air until they became viscous and sticky. When the sol was concentrated enough for fiber drawing, the

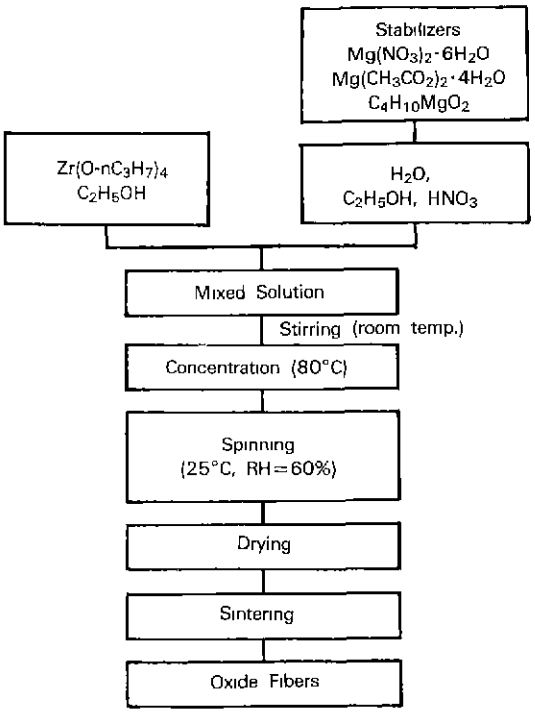

Fig. 1. Flow chart for preparing $MgO-ZrO_2$ fibers through Sol-Gel process.

zirconia gel fibers were drawn from the resultant yellowish viscous sol by immersing a glass rod of about 6 mm in diameter and pulling it up by hand in the laboratory (under 60% humidity at 25℃). We measured the viscosity changes of sol solution to investigate the viscosity changes depending on the amount of hydrolysis water and fiberazibility range of prepared sol solution and the viscosity as a function of aging time using LVTDV-II model viscometer. The drawn gel fibers were heated in air at a heating rate of 1℃/min in the range from room temperature to 1500℃, intermittently, held at various desired temperature for one hour, and then cooled in the furnace.

We analyzed the phase transformation and microstructure of heat-treated fibers using X-ray diffractometer, IR, Raman spectrophotometer, SEM, and microporosimeter.

Also, the tensile strength of fibers depending on the various heat treatment temperature and MgO sources was measured using an apparatus made in this laboratory to determine the mechanical properties of the fibers.

2.2. X-ray diffraction and vibrational spectroscopic analysis

To investigate the phase transformation relationships of $MgO-ZrO_2$ fiber depending on the amount of dopants and heat treatment temperature, the drawn fibers were heated at temperatures ranging from room temperature to 1500℃, and identified by means of PW1710 X-ray diffractometer (Philips. Co.) and RAMALOG-101 Raman spectrometer (Spex Co.). The Ni-filtered $CuK\alpha$ radiation was used as the X-ray source and the measurement conditions were as follows; 20 kV, 25 mA, 20° ~80° (2θ).

The Raman spectra of the fibers were recorded at the following conditions; resolution 1 cm^{-1}, slit width 80 μm. As an exciting line, the 514.5 nm line of an argon ion laser was used for these experiments and the incident laser power was 300 mW.

Also, when 12 mol% Mg(N) was added as a dopant, we measured IR spectrum to investigate the behavior of dopant in the gel fiber and the phase transformation depending on heat treatment temperatures.

A small amount of pulverized zirconia fiber was mixed with KBr powder and then pressed into a transparent pellet. IR transmission spectra were taken with the prepared specimens using MX-1 IR spectrometer (NICOLET Co.) with the following conditions; resolution 1 cm^{-1}, frequency range 400~4000 cm^{-1}, scanning no. 27.

2.3. Thermal analysis, microstructure, and tensile strength of fiber

To investigate the thermal properties of drawn $MgO-ZrO_2$ fibers, DT/TG analysis was conducted in air at a heating rate of 5℃/min using SDT1500 DT/TG analyzer (TA instrument Co.). Also, the microstructure of $MgO-ZrO_2$ fiber depending on the various heat treatment temperatures and MgO sources was investigated using X-650 scanning electron microscopy (Hitachi Co.) and autopore II 9220 Mercury Intrusion Porosimeter (Micromertics Co.). The tensile strength tester was made in this laboratory in accordance with Kamiya et al.[15].

3. Results and Discussion

3.1. Spinnability of $MgO-ZrO_2$ fiber

The reaction mechanism of hydrolysis-polycondensation for preparing zirconia using zirconium alkoxide has been reported by many researchers[16,17] and it is well known that it is hard to control the reaction rate because of rapid hydrolysis reaction even with small value of H_2O/alkoxide ratio. Even though there are many studies on the preparation of ZrO_2 fibers using zirconium alkoxide, only Kamiya[10] and Sakurai[11] proposed the polymerization mechanisms. From their reports, zirconia in zirconia sol solution must form the linear polymer structures in order for fiber to be formed from zirconium alkoxide and they reported H_2O /alkoxide molar ratio, and pH are important factors affecting the fiber fabrication. Kamiya et al.[10] and Kim et al.[18] proposed that the spinnability of the sol was accomplished by a H_2O/alkoxide molar ratio of 0.7~1.5 and below 1, respectively. On the other hand, Whang et al.[19] reported that the zirconia fiber can be drawn to the H_2O/alkoxide molar ratio of 3~4, if the pH of sol is below 1. Although more hydrolysis water is present than that required for the molar ratio of 3, the fibers can be drawn because the excess amounts of nitric acid suppressed the precipitation of zirconia at hydrolysis-polycondensation reaction, and also the linear polymeric structures formed in zirconia sol solution.

In the present work, we fabricated the MgO-ZrO_2 fibers on the basis of proper experimental conditions reported by Whang et al.[19] (H_2O/alkoxide molar ratio= 3~4, HNO_3/alkoxide molar ratio=1.3~1.5, initial pH= 0.8), and added Mg(N), Mg(A), Mg(E) as a dopant in the range of 10 to 18 mol%, and investigated the phase transformation depending on the amounts of dopants.

When the magnesium nitrate was added, the compositions and properties of sol solution for drawing MgO-ZrO_2 fiber are listed in Table 1. All of the fibers could be drawn in the whole range from 10 to 18 mol%, and in this case, H_2O/alkoxide molar ratio, HNO_3/alkoxide molar ratio, and initial pH was 3.1~3.6, 1.3~1.7, and 0.6, respectively. The molar ratio of ethanol varied in the range of 21.6 to 50.0, but had no effect on fiber drawing. Therefore, we fixed ethanol molar ratio at 21.6.

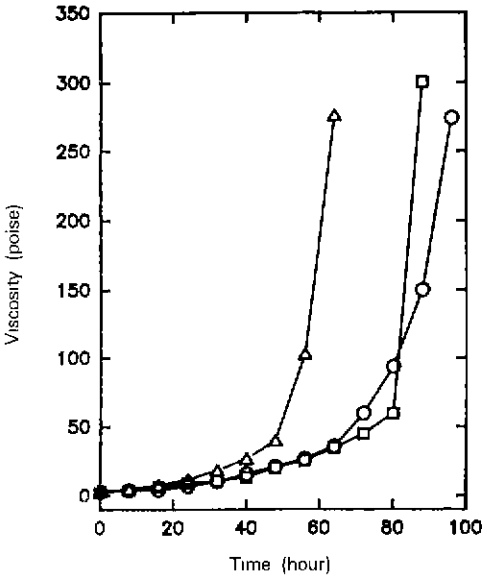

Fig. 2. Variation of the viscosity of 12MgO-88ZrO_2 (mol%) solution with the molar ratio $H_2O/Zr(O\text{-}nC_3H_7)_4$=3, 4, 5 as a function of time (△: 5; □: 4: ○: 3).

Fig. 2 illustrates the change in viscosity of 12 mol% Mg(N) doped ZrO_2 sol solutions with the molar ratios of $H_2O/Zr(O\text{-}nC_3H_7)_4$=3, 4, 5 versus aging time for the case in which the reaction temperature was kept constant at 80℃.

When the molar ratio of hydrolysis water is 3, we observed a slow increase in viscosity during the first

Table 1. Composition and Properties of Solution for the MgO-ZrO_2 System (MgO: $Mg(NO_3)_2 \cdot 6H_2O$)

Solution	Composition(molar ratio)				MgO (mol%)		Initial pH (25℃)	Reaction time at 80℃ /h	Fiber length (cm)
	$Zr(O\text{-}nC_3H_7)_4$	H_2O	C_2H_5OH	HNO_3	Cal.	Anal.			
10 MZ	1	3.10	21.6	1.64	10	9.5	0.6	5.30	50
12 MZ	1	3.40	21.6	1.73	12	11.5	0.5	5.30	50
14 MZ	1	3.35	21.6	1.60	14	—	0.6	6.00	40
16 MZ	1	3.57	21.6	1.70	16	—	0.6	6.00	30
18 MZ	1	3.33	21.6	1.33	18	—	0.6	6.00	30

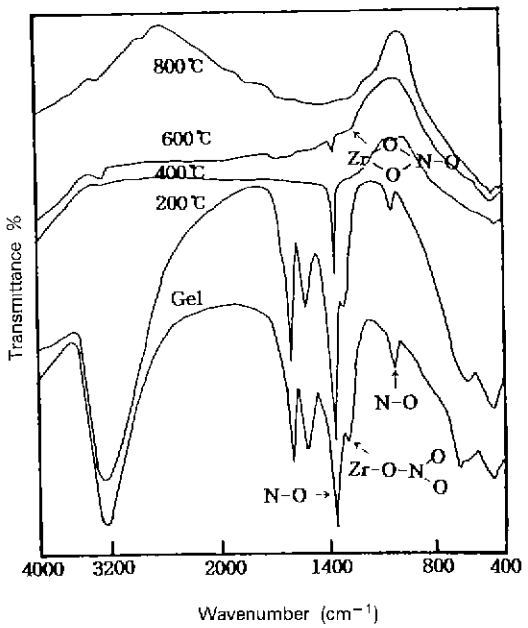

Fig. 3. FT-IR spectra of 12Mg(N) doped-ZrO_2 (in mol%) gel fibers heated to different temperature.

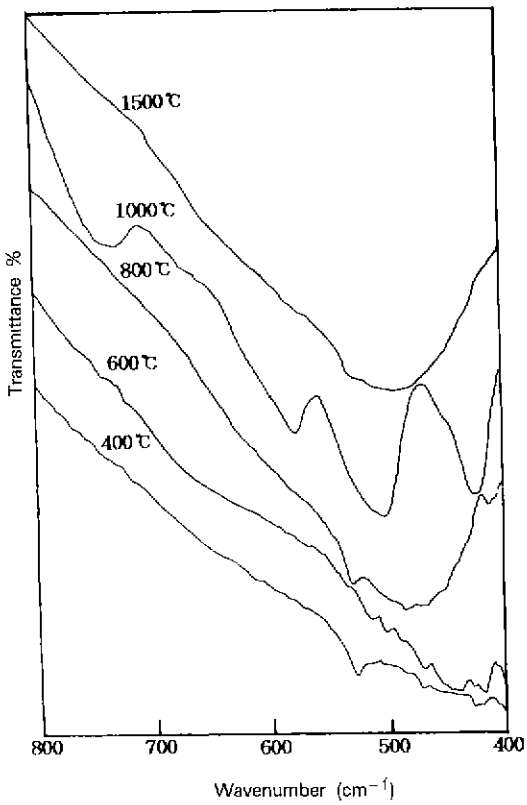

Fig. 4. FT-IR spectra of 12Mg(N) doped-ZrO_2 (in mol%) gel fibers as a function of sintering temperature.

60 hrs of aging time and then viscosity increased rapidly. When the molar ratio of hydrolysis water was increased to 5, the rapid increase in viscosity appeared after 40 hrs of aging time. Also, when the viscosity reached above 200 Poise, it was difficult to measure the viscosity because of gellation at the surface of sol solutions.

In the present experiment, we can produce the gel fibers of 10~50 μm diameter in the viscosity range between 20 and 70 Poise and observe the increase of fiber diameter as the viscosity increased.

3.2. Phase transformation studies of MgO-ZrO_2 fibers using X-ray diffraction and vibrational spectroscopy

3.2.1. IR spectrum of MgO-ZrO_2 gel fiber

In MgO-ZrO_2 fibers, we investigated the behaviors of MgO in fiber and the phase transformation relationships depending on the variation of sintering temperature by use of IR transmission spectroscopic analysis (Fig. 3 and Fig. 4).

Strong absorption peaks around 3200 cm^{-1} and 1600 cm^{-1} are ascribed to vibration of water molecules included in the samples. The nitrate groups in gel fibers may be present as ionic state (NO_3^-), monodentate (I), chelating (II) and/or bridging (III) groups[15,20].

Peaks around 1380 cm^{-1} and 1050 cm^{-1} are due to isolated NO_3^- ion corresponding to N-O stretching vibration and the shoulder peak around 1330 cm^{-1} and 1230 cm^{-1} are for NO_3^- groups covalently bonded to metal atoms in the forms such as monodentate and chelating. From the intensity of the nitrate peak, we conclude that a majority of NO_3^- groups is present in ionic state in the gel. As the temperature increases, NO_3^- ions disappear and then initial monodentate peak transforms to chelating or bridging represented around 1330 cm^{-1}.

IR results of MgO-ZrO_2 fibers sintered at 800℃ for 1 hr show the fact that all of nitrate peaks disappear completely and magnesium ions participate in a crystallization of zirconia.

Fig. 4 shows IR spectra of phase transformation of MgO-ZrO_2 fibers depending on the variation of sinter-

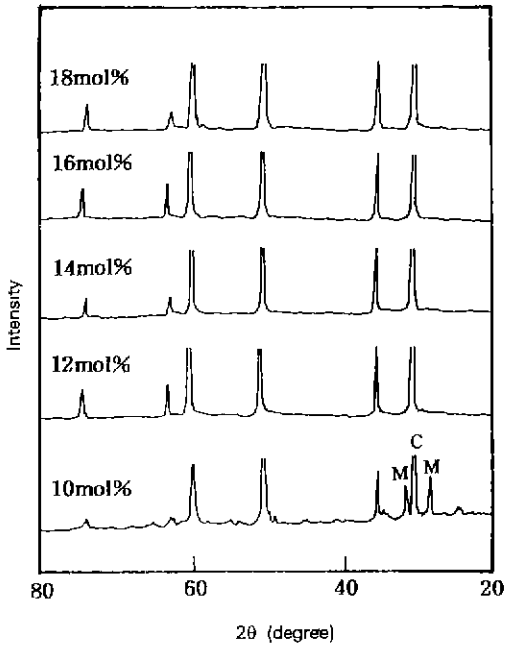

Fig. 5. X-ray diffraction patterns of ZrO_2 gel fibers taken as a function of MgO amount sintered at 1500℃ for 1 h (C: Cubic, M; Monoclinic).

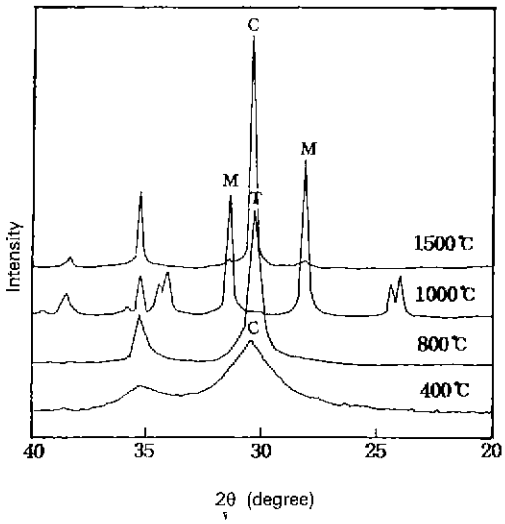

Fig. 6. X-ray diffraction patterns of 12Mg(N) fibers taken as a function of sintering temperatures (C: Cubic, T: Tetragonal, M: Monoclinic).

ing temperatures (400℃, 600℃, 800℃, 1000℃, and 1500℃) in 400~800 cm^{-1} ranges.

From the results of IR analysis of Y_2O_3-ZrO_2 fibers reported by Phillippi et al.[21], the peak of cubic is at 480 cm^{-1}, those of tetragonal at 365, 435, 510, 575 cm^{-1}, and those of monoclinic at 235, 270, 360, 375, 415, 445, 515, 620, 740 cm^{-1}, respectively. In the present work, the tetragonal peaks of fibers sintered at 800℃ for 1hr are around 441, 460, 470, 530 cm^{-1} and the monoclinic peaks of fibers sintered at 1000℃ are at 422, 502, 580, 730 cm^{-1} and cubic peak at around 482 cm^{-1} in 1500℃-sintered fibers.

3.2.2. Crystallization of MgO-ZrO_2 fibers depending on the variation of MgO amount and sintering temperature

XRD was used to study phase transformation with dopant concentration and sintering temperature. Fig. 5 represents the XRD patterns of MgO-ZrO_2 fibers depending on the variation of MgO amount in 10~18 mol% range sintered at 1500℃ for 1 hr.

In the case of 10 mol%, monoclinic and cubic peak coexist, and at 12 mol% monoclinic peak disappears and only cubic peak exists. After this, as the amount of MgO increases, the position and shape of peaks do not change.

Fig. 6 is the results of phase transformation of 12Mg (N) fibers depending on sintering temperatures in 20° ~40° (2θ) range.

Crystallization starts at 400℃. The crystalline species precipitating first was cubic as shown in d values (2.93) of main peak. In the case of 800℃-sintered fibers, the d value of main peak is 2.95 and represents similar to those of the metastable tetragonal. At 1000 ℃, the phase completely transformed to monoclinic. As the sintering temperature increases up to 1500℃, crystal phase changed to cubic (d value of main peak is 2.93) and coexists with a small amount of monoclinic. The sequence of phase transformations with the thermal evolution of MgO-ZrO_2 (12 mol% Mg(N)) fiber is determined in the following way: MgO-ZrO_2, amorphous gel→cubic (400℃)→metastable tetragonal (800 ℃)→monoclinic (1000℃)→cubic(trace of monoclinic) (1500℃). This is in agreement with observations reported by Kundu et al.[20].

Fig. 7 represents XRD patterns of phase transformation of 12Mg(N), 12Mg(A), and 12Mg(E) fibers with different MgO sources sintered up to 1500℃ in 20°~ 80° (2θ) range. The phase transformation in all of these compositions represents the same tendency. But,

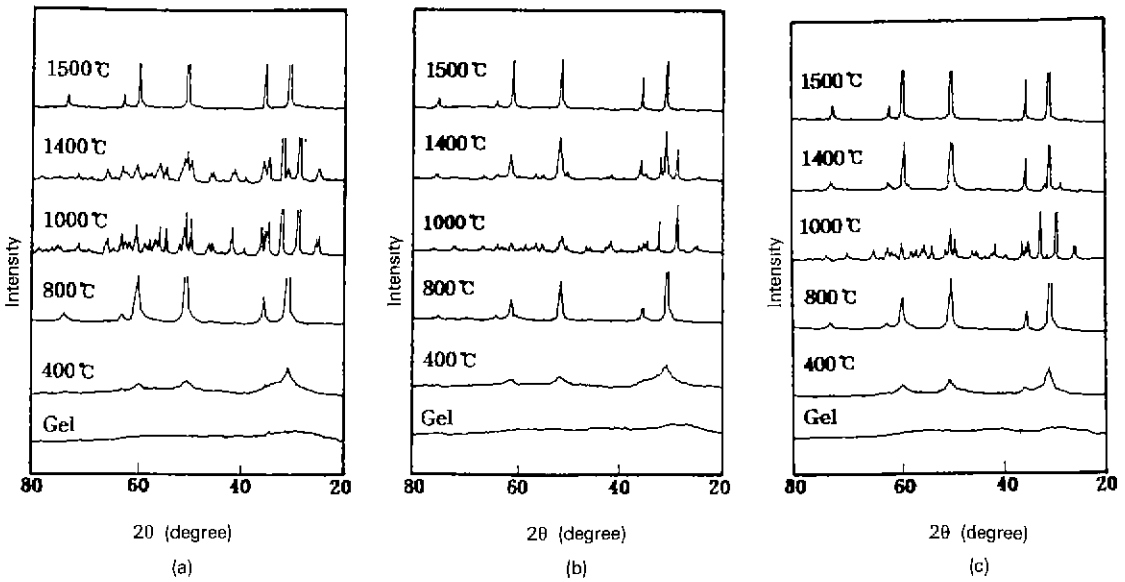

Fig. 7. X-ray diffraction patterns of ZrO_2 gel fibers taken as a function of sintering temperatures for (a) Mg(N), (b) Mg(A), and (c) Mg(E).

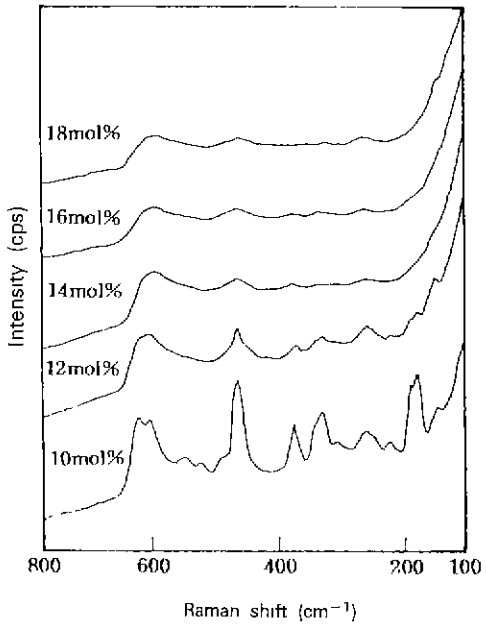

Fig. 8. Raman spectra of ZrO_2 gel fibers taken as a function of MgO amount sintered at 1500℃ for 1 h.

at 1400℃, the ratios of cubic to monoclinic exhibited as follows: Mg(E)>Mg(A)>Mg(N).

The symmetries of the Raman bands corresponding to the various phases have been discussed earlier[20-22]. As it can be seen, the Raman spectra reflect the effects of increasing MgO concentrations.

Fig. 8 shows Raman spectra of ZrO_2 fibers which contain Mg(N) in 10~18 mol% range.

In the case of 10 mol%, Raman spectra exhibits a mixture of monoclinic and cubic phase. At 12 mol%, the intensities of the characteristic monoclinic peaks decrease rapidly and only traces of monoclinic phase exist. This result is in disagreement with the XRD result which shows no monoclinic phase at 12 mol% MgO. This result clearly demonstrates that the sensitivity with which the Raman spectra are capable of detecting the monoclinic phase in the presence of cubic phase.

From 14 mol%~18 mol% range, the shape of the broad continuum of Raman band varies little with concentrations of MgO. In this region, disordered cubic phase exhibit a broad, poorly defined maxima at 618, 262, and 146 cm^{-1}. It is apparent from the Raman spectra of the disordered cubic zirconia that this solid solution behaves more like an amorphous than a crystalline compound. This result is in accordance with the CaO-ZrO_2 system with massive point defects studied by Keramidas et al.[22].

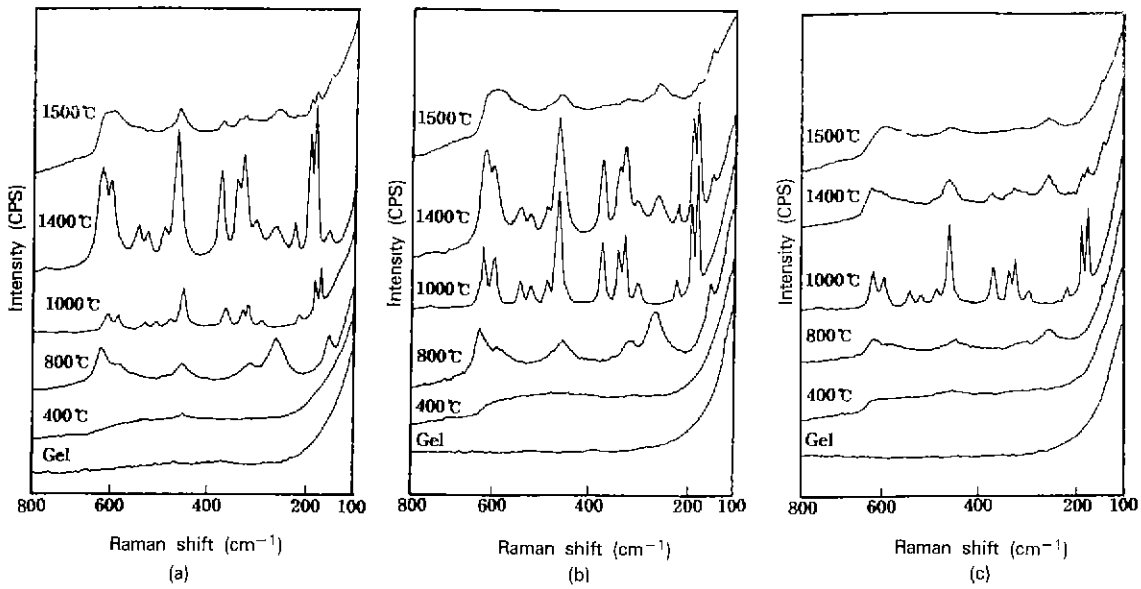

Fig. 9. Raman spectra of ZrO_2 gel fibers taken as a function of sintering temperatures for (a) Mg(N), (b) Mg(A), and (c) Mg(E).

The phase transformation of 12Mg(N), 12Mg(A), and 12Mg(E) fibers depending on the variation of sintering temperatures by use of Raman spectroscopic analysis is shown in Fig. 9.

All of gel fibers start to crystallize at 400℃. At 800 ℃, we can observe tetragonal phase as the first precipitating crystal species and six Raman active modes predicted from the group theory are all present at 149, 265, 322, 467, 604, and 644 cm^{-1}. As the sintering temperature is raised up to 1000℃, all of the characteristic tetragonal peaks disappear and doublet of monoclinic peaks start to develop. From the group theory, monoclinic phase is predicted to have 18 Raman active modes, but only 13 Raman active modes are observed in this study. At 1400℃, mainly, monoclinic phase exists, but, small amount of cubic phase coexist. At 1500 ℃, the shape and intense band of the well ordered monoclinic phase is transformed to a very broad, ill-defined band of disordered cubic phase. This agrees with the results from XRD and IR spectroscopic studies. Also, in the case of 12Mg(N) fibers, the characteristic monoclinic doublet at 181 and 192 cm^{-1} is still present very weakly.

12Mg(A) and 12Mg(E) fibers exhibit the same tendency with 12Mg(N) fibers.

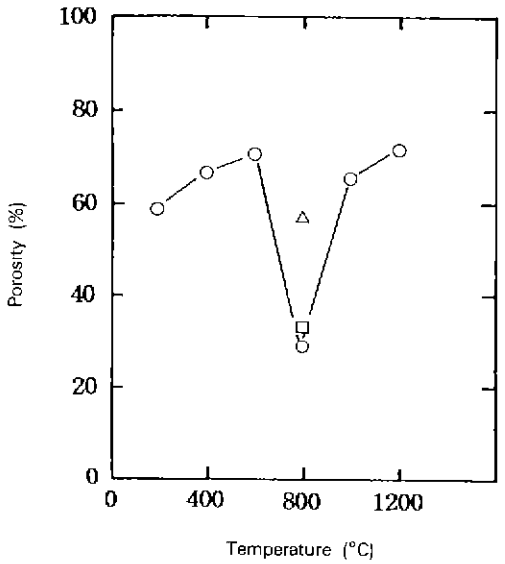

Fig. 10. Porosity of 12Mg(N) fibers sintered at different temperatures and 12Mg(A) and 12Mg(E) fibers sintered at 800℃ for 1 h (○: 12Mg(N), □: 12Mg(A), △: 12Mg(E)).

3.3. The properties and microstructures of MgO-ZrO_2 fibers

Fig. 10 represents the variation of the microporosity

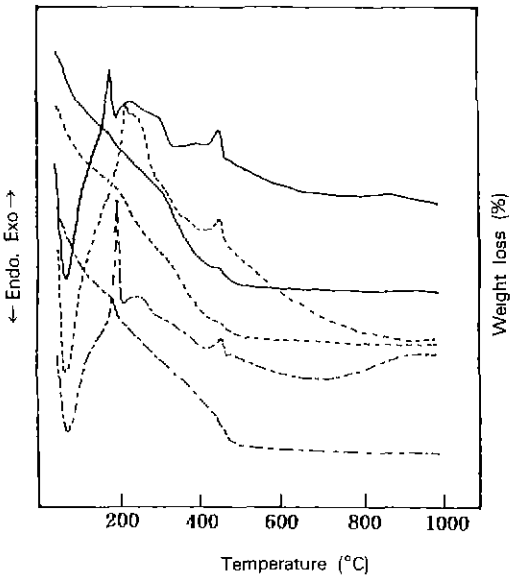

Fig. 11. DT/TG analysis of ZrO_2 gel fibers for 12Mg (N), 12Mg(A), and 12Mg(E) (—: 12Mg(N); ---: 12Mg(A); -·-: 12Mg(E)).

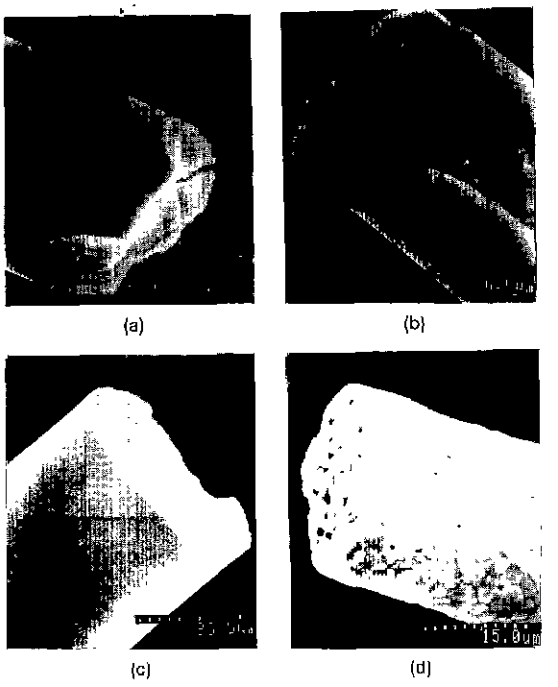

Fig. 12. Scanning electron micrographs of 12Mg(N) fibers for (a) gel, (b) 800℃, (c) 1000℃, and (d) 1500℃.

of 12 mol% Mg(N)-ZrO_2 fibers with the sintering temperatures (200℃, 400℃, 800℃, 1000℃, and 1200℃) and also with the various MgO sources (12Mg(N), 12 Mg(A), and 12Mg(E) sintered at 800℃ for 1 hr).

In the porosity variation depending on the sintering temperatures, the high porosity before 800℃ is due to the decomposition of organic materials and nitrate in 12Mg(N) gel fibers. Since the decomposition of organic materials and nitrate are completed at 800℃, the fibers have a minimum porosity. At 1000℃, the increasing porosity was due to the coalescence of pores between grains by the rapid sintering of grains in gel fibers.

Also, in the cases of the variation of microporosity with the MgO sources, 12Mg(N) fibers have the lowest porosity, that is, it is due to the rapid decomposition of acetate and ethylate producing large pores in 12Mg (A) and 12Mg(E) fibers at low temperature, while the slow decomposition of nitrate produced small pores in 12Mg(N) fibers.

Fig. 11 shows the DT/TG analysis of MgO-ZrO_2 fibers depending on the variation of MgO sources such as 12Mg(N), 12Mg(A), and 12Mg(E).

All of fibers represent the same tendancy. That is, large endothermic peak observed below 100℃ are due to the evaporation of alcohol and water remaining in the gel. All of fibers exhibit the exothermic peaks due to the decomposition of organic materials in temperature range of 200~300℃. In the case of 12Mg(E), the sharp exothermic peak around 200℃ is due to the more decomposition of organic materials than 12Mg(N) or 12Mg(A). A large portion of acetate or nitrate groups incorporated into gel structure is thermally decomposed at 350~450℃, leaving micropores.

All of fibers show a small exothermic peak around 450℃ which is attributed to the crystallization of gel fibers.

Also, all of fibers exibited about 52% weight loss.

The difference in thermal evoulation such as decomposition temprature and rate among the gel fibers depend on the variation of MgO sources.

Accordingly, the difference in thermal behavior of gel fibers produce the difference in pore structure which in turn, affect the mechanical strength of resultant fibers.

Fig. 12 shows SEM photographs of the microstructure of 12Mg(N) gel fiber, 800℃-, 1000℃-, and 1500℃-

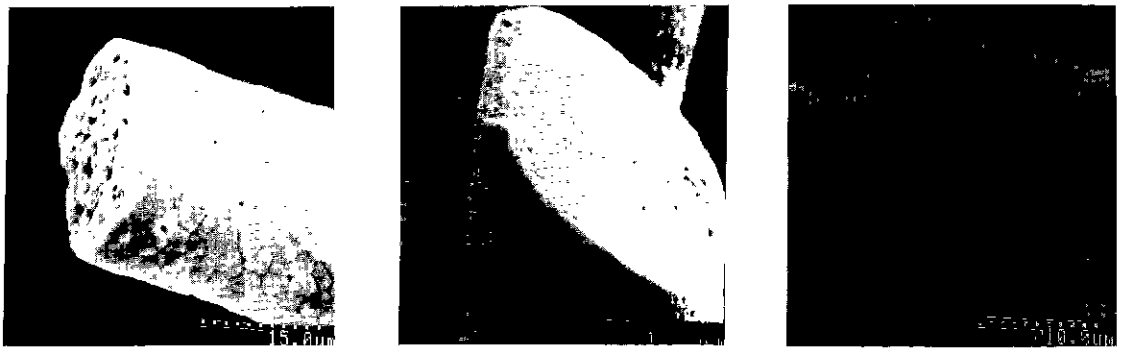

Fig. 13. Scanning electron micrographs of 12Mg(N), 12Mg(A), and 12Mg(E) fibers sintered at 1500℃ for 1 h.

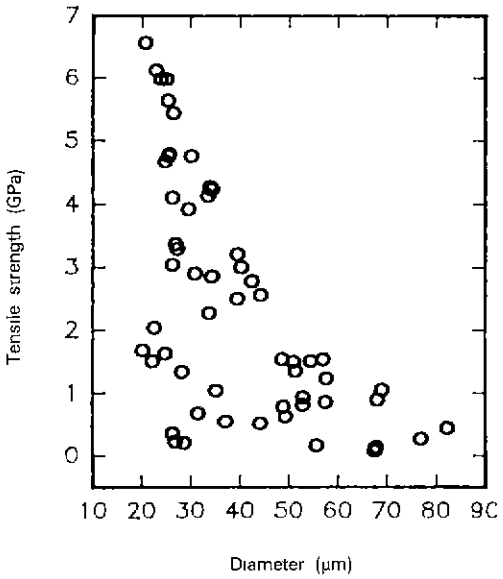

Fig. 14. Tensile strength of 12Mg(N) fibers sintered at 800℃ for 1 h.

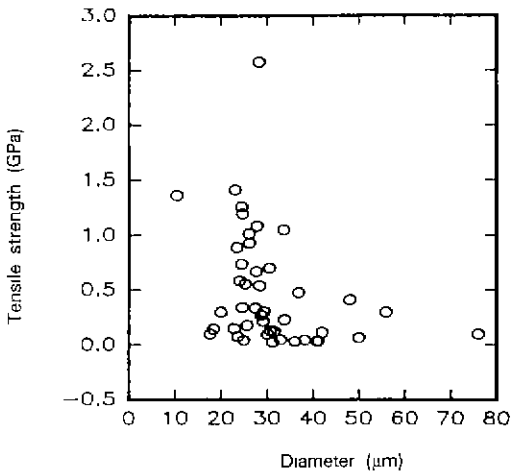

Fig. 15. Tensile strength of 12Mg(N) fibers sintered at 1000℃ for 1 h.

treated fibers, respectively.

From SEM results, the diameter and cross-section represent the various shapes which are related with the variation of viscosity at fiber drawing. That is, the fibers have a small diameter and a round cross-section in low viscous sol solutions, while the fibers have a large diameter and not-round cross-section in high viscous sol solutions.

In the case of 12Mg(N), 800℃-, and 1000℃-heat treated fibers retain very smooth surface and fracture surface. However, average grain size of fiber sintered at 1500℃ for 1hr increases to approximately 5 μm and shows many pores between grains. It is believed that small pores are coalesced in grain boundary due to the rapid grain growth of fine grains in fiber at high temperature and formed the continuous pore trail to the fiber surface. These results are in good agreement with those of Sim et al.[23].

Fig. 13 shows SEM photographs of the surface and fracture surface of 12Mg(N), 12Mg(A), and 12Mg(E) fibers sintered at 1500℃ for 1 hr.

All of fibers show the rapid grain growth and retain many pores.

3.4. The tensile strength measurement of MgO-ZrO_2 fibers

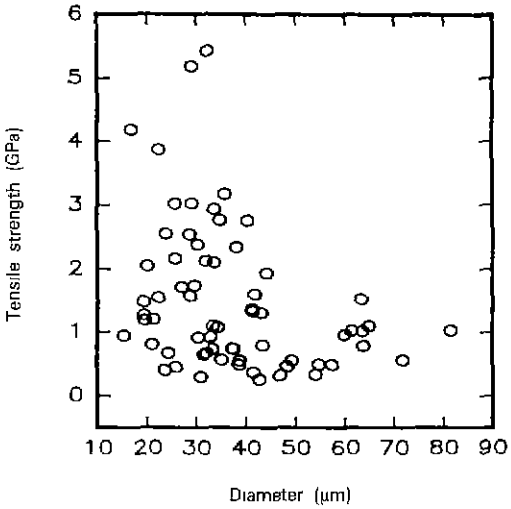

Fig. 16. Tensile strength of 12Mg(A) fibers sintered at 800℃ for 1 h.

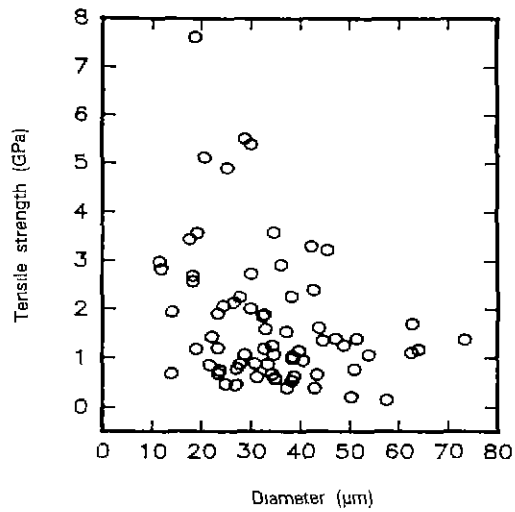

Fig. 17. Tensile strength of 12Mg(E) fibers sintered at 800℃ for 1 h.

To investigate the mechanical properties of 12Mg(N) fibers, we measured the tensile strength of fibers sintered at 800℃ and 1000℃ for 1 hr, respectively (Fig. 14 and Fig. 15).

Since hand-drawn fibers do not have a constant diameter and a unique shape in cross-section as shown in SEM results, tensile strength and fiber diameter are scattered.

Average tensile strength of 800℃-treated 12 mol% Mg(N) fibers is about 4.0 GPa at diameter of 20~30 μm, while that of 1000℃-treated fibers decreases to 0.7 GPa at the same diameter range. This is due to the phase transformation from tetragonal phase (800℃) to monoclinic phase (1000℃) as observed by XRD and Raman spectroscopy and the lowest porosity of 800℃-treated fibers by microporosity measurement.

Tensile strengths of 12Mg(N), 12Mg(A), and 12Mg(E) fibers sintered at 800℃ for 1hr are shown in Fig. 14, Fig. 16, and Fig. 17.

Average tensile strength of 12Mg(A) and 12Mg(E) fibers is about 2.0 GPa and 1.9 GPa, respectively and they have a lower tensile strength than 12Mg(N) fibers at diameter range of 20~30 μm. The more rapid removal of acetate and ethylate in 12Mg(A) and 12Mg(E) fibers than nitrate in 12Mg(N) fibers and many pores play the important role of decreasing the tensile strength of the fibers.

4. Conclusions

In the present study, we succeeded in fabricating $MgO-ZrO_2$ fibers by sol-gel process using $Zr(O\text{-}nC_3H_7)_4$-H_2O-C_2H_5OH-HNO_3 solutions and different MgO sources.

Following results were obtained.

1) $MgO-ZrO_2$ fibers could be hand drawn from the solutions with pH lower than 0.6, and concentrated at 80℃. The gel fibers and sintered fibers have diameter of 10 to 50 μm and length of 30 to 50 cm.

Also, no important differences in spinnability were observed depending on the origin of MgO and its amount.

2) The analysis of XRD and Raman spectra of Mg(N) fibers containing from 10 to 18 mol% magnesium nitrate sintered at 1500℃ for 1hr, we conclude that monoclinic phase and cubic phase coexist at 10~12 mol%, while only cubic phase is present from 14 mol%.

3) When the MgO contents in $MgO-ZrO_2$ fibers are fixed at 12 mol% and MgO sources are varied (Mg(N), Mg(A), and Mg(E)), the XRD, IR, and Raman spectroscopic studies shows the following phase transformation; cubic→metastable tetragonal→monoclinic→coexistance of monoclinic and cubic→cubic.

4) From the microporosity results of 12Mg(N) fibers depending on sintering temperatures, 800℃-treated fi-

bers represent the lowest porosity.

Also, as the MgO sources are varied to 12Mg(N), 12Mg(A), and 12Mg(E) sintered at 800℃ for 1hr, 12Mg (N) fibers represent the lowest porosity. It is thought to be due to the more rapid decomposition of acetate and ethylate than nitrate in fiber.

5) The tensile strength of 800℃-treated 12Mg(N) fibers is 4.0 GPa at diameter of 20 to 30 μm, while that of 1000℃-treated fibers is 0.7 GPa at the same diameter range. It is due to the phase transformation from tetragonal (800℃) to monoclinic (1000℃).

Also, the tensile strength of 12Mg(N), 12Mg(A), and 12Mg(E) fibers sintered at 800℃ for 1hr is 4.0, 2.0, and 1.9 GPa at diameter of 20 to 30 μm.

Acknowledgement

We gratefully acknowledge the financial support for this work from The Korea Research Foundation.

REFERENCES

1. Advances in Ceramics, Vol. 3, Science and Technology of Zirconia I, Edited by A.H. Heuer and L.W. Hobbs, Am. Ceram. Soc., Columbus, OH (1981).
2. R. Stevens, "Zirconia and Zirconia Ceramics," pp. 12~24, Magnesium Elektron Pub. No. 113 (1986).
3. R.C. Garvie, R.H. Hannink, and R.T. Pascoe, "Ceramic Steel?," *Nature*, **258**, 703-04 (1975).
4. P.A. Janeway,"PSZ-A Breakthrough in Toughness," *Ceram. Industry*, **122**, 40-45 (1984).
5. R.R. Hughan and R.H. Hannink, "Precipitation During Controlled Cooling of Magnesia-Partially-Stabilized Zirconia," *J. Am. Ceram. Soc.*, **69**(7), 556-563 (1986).
6. T.J. Hine, M.K. Ferber, and D.W. Leigh, "Time-Dependent Mechanical Behavior of MgO-PSZ Ceramics," Advanced Ceramic Materials, **3**(1), 80-87 (1988).
7. P.A. Vityaz, I.L. Fyodorova, I.N. Yermolenko, and T.M. Ulyanova, "Synthesis of Alumina and Zirconia Fibers," *Ceramics International*, **8**(2), 46-48 (1983).
8. D.B. Marshall, F.F. Lange, and P.D. Morgan, "High Strength Zirconia Fibers," *J. Am. Ceram. Soc.*, **70**(8), c-187~c-188 (1987).
9. T. Kokubo, Y. Teranish, and T. Maki, "Preparation of Amorphous ZrO_2 Fibers by Unidirectional Freezing of Gel," *J. Non-cryst. Solids*, **56**, 411 (1983).
10. K. Kamiya, T. Yoko, K. Tanaka, and H. Ito, "Preparation of Fiberous ZrO_2 and CaO-ZrO_2 from Zirconium Alkoxide by Sol-Gel Method," *Yogyo-Kyokai-Shi*, **95** (12), 1157 (1987).
11. C. Sakurai, T. Fukui, and M. Okuyama, "Hydrolysis Method for Preparing Zirconia Fibers," *Ceramic Bulletin*, **70**(4), 673 (1991).
12. S. Horikiri, "ジルコニア繊維の 製造法," Japanese Pat. 74-134928 (1974).
13. J.E. Blaze, "Process of Manufacturing Refractory Fibers," *US Pat. 3,322,865* (1967).
14. I.N. Yermolenko, T.M. Ulyanova, P.A. Vityaz, and I.L. Fyodorova, "Structure of Stabilized Zirconium Dioxide Fibers," pp. 367-375 in Zirconia '88, Advances in Zirconia Science and Technology, Edited by S. Meriani and C. Palmonari, Elsevier Applied Science, 1989.
15. K. Kamiya et al., "Sol-Gel Derived CaO- and CeO_2-Stabilized ZrO_2 Fibers-Conversion Process of Gel to Oxide and Tensile Strength," *J. Eur. Ceram. Soc.*, **7**, 295 (1991).
16. K.S. Mazdiyasni, C.T. Lynch, and J.S. Smith, "Preparation of Ultra-High-Purity Submicron Refractory Oxides," *J. Am. Ceram. Soc.*, **48**(7), 372 (1965).
17. B.E. Yoldas, "Zirconia Oxides Formed by Hydrolytic Condensation of Alkoxides and Parameters that Affects Their Morphology," *J. Mat. Sci.*, **21**, 1080 (1986).
18. S. Kim, S.S. Kim, and W.C. LaCource, "ZrO_2 Ceramic Fiber Fabrication by Sol-Gel Processing," *J. of Korean Ceram. Soc.*, **27**(6), 824 (1990).
19. C.M. Whang, H.T. Eun, and H.K. Kwon, "Fabrication of Y_2O_3-ZrO_2 and CaO-ZrO_2 Fibers by Sol-Gel Process and Their Phase Characterization by Raman Microprobe," *J. of Korean Ceram. Soc.*, **31**(1), 104 (1994).
20. K. Nakamoto, Infrared and Raman Spectra of Inorganic and Coordination Compounds, John Wiley & Sons, NY, 1963.
21. C.M. Plillippi and K.S. Mazdiyasni, "Infrared and Raman Spectra of Zirconia Polymorphs," *J. Am. Ceram. Soc.*, **54**(5), 254-258 (1971).
22. V.G. Keramidas and W.B. White, "Raman Scattering from $Ca_xZr_{1-x}O_{2-x}\square_x$, A System with Massive Point Defects," *J. Phys. Chem Solids*, **14**, 1873 (1975).
23. S.M. Sim and D.C. Clark, "Preparation of Zirconia Fibers by Sol-Gel Method," *Ceram. Eng. Sci. Proc.*, **10**(9-10), 1271 (1989).
24. P. Kundu, D. Pal, S. Sen, "Preparation and Thermal Evolution of Sol-Gel Derived Transparent ZrO_2 and MgO-ZrO_2 Gel Monolith," *J. Mater. Sci.*, **23**, 1539 (1988).